Resonances of a Nonlinear Single-Degree-of-Freedom System with Time Delay in Linear Feedback Control

Atef F. El-Bassiouny[a] and Salah El-Kholy[b]

[a] Faculty of Science, Mathematics Department, Benha University, Benha 13518, Egypt
[b] Department of Mathematics, Faculty of Science, Menoufia University, Shebin El-kom, Egypt

Reprint requests to A. F. E.-B.; E-mail: atef_elbassiouny@yahoo.com

Z. Naturforsch. **65a,** 357 – 368 (2010); received January 24, 2008

The primary and subharmonic resonances of a nonlinear single-degree-of-freedom system under feedback control with a time delay are studied by means of an asymptotic perturbation technique. Both external (forcing) and parametric excitations are included. By means of the averaging method and multiple scales method, two slow-flow equations for the amplitude and phase of the primary and subharmonic resonances and all other parameters are obtained. The steady state (fixed points) corresponding to a periodic motion of the starting system is investigated and frequency-response curves are shown. The stability of the fixed points is examined using the variational method. The effect of the feedback gains, the time-delay, the coefficient of cubic term, and the coefficients of external and parametric excitations on the steady-state responses are investigated and the results are presented as plots of the steady-state response amplitude versus the detuning parameter. The results obtained by two methods are in excellent agreement.

Key words: Nonlinear Single-Degree-of-Freedom; Resonances; Time Delay; Perturbation Methods; Fixed Points; Stability.

1. Introduction

Nonlinear systems may exhibit considerably complex behaviour such as changes in the stability of engineering systems which explains the reason why research in the area of dynamics and its control of nonlinear systems has received great attention in the past two decades [1 – 3].

Especially the nonlinear system with time delays has been an active topic of research over the past decades [4 – 22]. Plaut and Hsieh [4] numerically analyzed the steady-state response of a nonlinear one-degree-of-freedom mechanism with time delays for various sets of parameters by a Runge-Kutta numerical integrations procedure. It was found that the response might be periodic, chaotic or unbounded. By the method of multiple scales, Plaut and Hsieh [5] studied the effect of damping time delay on nonlinear structure vibrations and analyzed six resonance conditions. They gave the results in a number of figures for the steady-state response amplitude versus the excitation frequency and amplitude. Abdel-Rohman [6] considered the effect of small time delay on the stability of a distributed parameter structure with the velocity feedback using Taylor's series expansion and neglecting the second-order terms. Chung et al. [7] also conducted experimental studies on an multi-degree-of-freedom (MDOF) system with equal delay times. Pu and Kelly [8] used the frequency response analysis for a single-degree-of-freedom (SDOF) system with equal delay times to find the maximum allowable time delay beyond which the system becomes unstable. In their analysis both steady-state and transient behaviours were considered. Palkovics and Venhovens [9] investigated the stability and possible chaotic motions in the controlled wheel suspension system. Agrawal et al. [10] performed a stability analysis for an SDOF model with equal delay times and found a closed form solution for the critical delay time or the maximum allowable time delay. Moiola et al. [11] studied the degeneracy conditions of a Hopf bifurcation in an autonomous nonlinear feedback system with time delay using the frequency-domain approach. Two simple examples of nonlinear autonomous delayed systems were presented; the computation of the two periodic branches near a degenerate Hopf bifurcation point was given. Xu and Jiang [12] examined the global bifurcation characteristics of a forced van der Pol oscillator. Yabuno [13] investigated the bifurcation control of a parametrically excited Duffing system using combined linear-plus-nonlinear feedback control. Yabuno [14] proposed also a control law based on linear velocity feedback and linear and cubic velocity feedback. His studies demonstrated that nonlinear position feedback reduces the response amplitude in the parametric excitation-response curve, while velocity feedback stabilizes the trivial solution in the frequency-response curve. Hu et al. [15] investigated the primary and subharmonic resonances of a harmonically forced Duffing oscillator with time delay state feedback. The concept of an equivalent damping was proposed and an appropriate choice of the feedback gains and time delay was discussed from the viewpoint of vibration control. Hu and Wang [16] analyzed the stability of a damped SDOF system with two time delays in state feedback. Atay [17] analyzed the effects of delayed position feedback on the response of a van der Pol oscillator. Hegazi et al. [18] used the linear and nonlinear feedback control techniques to suppress chaos. The controlled system is stable under some conditions on the parameter of the system. Ji [19] studied the saddle-node bifurcation control of a forced SDOF Duffing oscillator with damping for time delay. Maccari [20] investigated the parametric resonance of a van der Pol oscillator under state feedback control with time delay. In [21, 22], Ji and Leung discuss the primary, subharmonic and superharmonic resonances of a Duffing system with damping under linear feedback control with two time delays and the bifurcation control of a parametrically excited Duffing system, respectively. Fofana and Ryba [23] analyzed the stability behaviour of delay differential equations chatter instability in machining operations. Peng [24] investigated effective approaches to explore rich dynamics of delay differentials. Park [25] analyzed the design of a dynamic controller for neutral differential systems with delay in control input. Liu and Yuan [26] investigated the stability and bifurcation in a harmonic oscillator with delays. Yassen [27] studied the controlling chaos and synchronization of a new chaotic system using linear feedback control. Wang and Liu [28] investigated the stability and bifurcation analysis in a magnetic bearing system with time delays. El-Bassiouny [29] analyzed fundamental and subharmonic resonances of harmonic oscillations with time delay state feedback. El-Bassiouny [30] studied the vibration control of a cantilever beam with time delay state feedback. Sun et al. [31] investigated the effects of time delays on bifurcation and chaos in a non-autonomous system with multiple time delays. El-Bassiouny [32] investigated the stability and oscillation of two coupled Duffing equations with time delay state feedback. El-Bassiouny et al. [33 – 42] used the method of averaging and the method of multiple scales to investigate the response of SDOF and MDOF systems.

In the present paper, the nonlinear dynamical behaviour of a harmonicly excited nonlinear SDOF system with time delay is analyzed under primary and subharmonic resonance conditions. The equation of motion is assumed to has the following form:

$$\ddot{y}+\omega_0^2 y=\varepsilon[c_1\dot{y}(t-\tau)+c_3y^3+c_4y\cos\omega t + (c_5+c_6y^3)\sin\omega t]. \tag{1}$$

This system is related to the model for many applications, such as active vehicle suspension systems when the nonlinearity in the tires is considered.

2. Averaging Method

The method of averaging [43, 44] is based on the assumption that small perturbations, such as weak nonlinearities or light damping, cause (slow-frequency) variations in the response of a system. The fast (high-frequency) variations due to the perturbations are assumed to be insignificant. Essentially, the averaging approximation yields a simplified mathematical representation of the dynamics of the system by smoothing away these fast variations. Thus, it is of basic importance that the components which make up the response be correctly classified either as fast or slow.

Usually, the response of each mode is assumed to be of the form $u_n=a_n(t)\cos(\omega_n t+\beta_n)$, where the $a_n(t)$ and $\beta_n(t)$ are assumed to vary slowly. The equations of motion are then transformed into a system of first-order equations for the $a_n(t)$ and $\beta_n(t)$ and, after some manipulation, the equations are integrated with respect to the time t from 0 to $\frac{2\pi}{\omega_n}$. The averaging approximation consists of the treatment of the slowly varying quantities as constants because they change very little over the period of integration.

An alternative strategy for the low-frequency mode can be developed as follows. Neglecting the damping, nonlinearities, and the external and parametric excitations, one can write the solution of (1) as

$$y=a(t)\cos(\omega_0 t+\beta), \tag{2}$$

where a and φ are constants. It follows from (2) that

$$\dot{y}=-\omega_0 a\sin(\omega_0 t+\varphi). \tag{3}$$

For $\varepsilon \neq 0$, we assume that the solution of (1) is still given by (2). But as a and β vary with the time t, we obtain

$$\dot{y} = -\omega_0 a \sin(\omega_0 t + \varphi) + \dot{a}\cos(\omega_0 t + \varphi) - a\dot{\beta}\sin(\omega_0 t + \varphi). \tag{4}$$

Comparing (4) with (3), we conclude that

$$\dot{a}\cos(\omega_0 t + \varphi) - a\dot{\varphi}\sin(\omega_0 t + \varphi) = 0. \tag{5}$$

Differentiating (3) with respect to t, we have

$$\ddot{y} = -\omega_0^2 a\cos(\omega_0 t + \varphi) - \omega_0 \dot{a}\sin(\omega_0 t + \varphi) - \omega_0 a\dot{\varphi}\sin(\omega_0 t + \varphi). \tag{6}$$

Inserting y, $\dot{y}$, and $\ddot{y}$ from (2), (3), and (6) into (1), we obtain

$$\begin{aligned} &\omega_0 \dot{a}\sin\psi - \omega_0^2 a\cos\psi - \omega_0 a\dot{\varphi}\cos\psi \\ &+\varepsilon[-c_1 a\omega_0 \sin\psi + c_2 a\cos\psi \\ &\quad - c_3 a^3\cos^3\psi - c_4 a\cos\psi\cos\omega t \\ &\quad - \cos\omega t(c_5 + c_6 a^3\cos^3\psi)] = 0, \end{aligned} \tag{7}$$

where

$$\psi = \omega_0 t + \varphi. \tag{8}$$

Solving (5) and (7) for $\dot{a}$ and $\dot{\varphi}$ and using the trigonometric identities gives the following variational equations:

$$\begin{aligned} \omega_0\dot{a} = \varepsilon\Bigg[&-\frac{1}{2}a\omega_0^2\sin 2\psi - c_1 a\omega_0\left(\frac{1}{2}(1-\cos 2\psi)\cos\omega_0\tau + \frac{1}{2}\sin 2\psi\cos\omega_0\tau\right) \\ &-\frac{1}{4}c_3 a^3\left(\sin 2\psi + \frac{1}{2}\sin 4\psi\right) - \frac{1}{4}c_4 a(\sin(\omega t + 2\psi) + \sin(\omega t - 2\psi)) \\ &-\frac{1}{2}c_5(\cos(\omega t - \psi) - \cos(\omega t + \psi)) - c_6 a^3\left\{\left(\frac{1}{8}\cos(\omega t - 2\psi) - \frac{1}{8}\cos(\omega t + 2\psi)\right)\right. \\ &\left.+\frac{1}{16}\cos(\omega t - 4\psi) + \frac{1}{16}\cos(\omega t + 4\psi)\right\}\Bigg], \end{aligned} \tag{9}$$

$$\begin{aligned} \omega_0\dot{\varphi} = \varepsilon\Bigg[&-\frac{1}{2}a\omega_0^2\sin 2\psi - c_1 a\omega_0\left(\frac{1}{2}\sin 2\psi\cos\omega_0\tau + \frac{1}{2}(1+\cos 2\psi)\sin\omega_0\tau\right) \\ &-\frac{1}{4}c_3 a^3\left(\frac{3}{2} + 2\cos 2\psi + \frac{1}{2}\cos 4\psi\right) - c_4 a\left(\frac{1}{2}\cos\omega t + \frac{1}{4}\cos(\omega t + 2\psi) + \frac{1}{4}\cos(\omega t - 2\psi)\right) \\ &-\frac{1}{2}c_5(\sin(\omega t + \psi) + \sin(\omega t - \psi)) - c_6 a^3\left\{\left(\frac{3}{8}\sin\omega t + \frac{1}{4}\sin(\omega t + 2\psi) + \frac{1}{4}\sin(\omega t - 2\psi)\right)\right. \\ &\left.+\frac{1}{16}\sin(\omega t + 4\psi) + \frac{1}{16}\sin(\omega t - 4\psi)\right\}\Bigg]. \end{aligned} \tag{10}$$

Two cases of resonances are considered in the following sections.

2.1. Primary Resonance

For obtaining the averaging equations corresponding to the primary resonance ($\omega = \omega_0 + \varepsilon\sigma$), we retain only the constant terms and the terms of small frequency in (9) and (10). Then we get

$$\omega_0\dot{a} = \varepsilon\left[-c_1 a\omega_0\cos\omega_0\tau - \frac{1}{2}c_5\cos\gamma_1\right], \tag{11}$$

$$\omega_0 a\dot{\varphi} = \varepsilon\left[-\frac{1}{2}c_1 a\omega_0\sin\omega_0\tau - \frac{3}{8}c_3 a^3 - \frac{1}{2}c_5\sin\gamma_1\right], \tag{12}$$

where

$$\gamma_1 = (\omega - \omega_0)t - \varphi = \varepsilon\sigma t - \varphi. \tag{13}$$

Obviously, the presence of the feedback gains and time delay modifies the averaged equations by adding terms that are relevant to feedback control. Thus, it is possible to achieve the desirable behaviour if the feedback is deliberately implemented.

Steady-state solutions of (1) for the primary resonance correspond to the fixed points of (11) and (12), which can be obtained by setting $\dot{a} = \dot{\gamma}_1 = 0$. That is

$$\frac{1}{2}c_1 a\cos\omega_0\tau + \frac{1}{2\omega_0}c_5\cos\gamma_1 = 0, \tag{14}$$

$$\sigma a + \frac{1}{2}c_1 a\sin\omega_0\tau + \frac{3}{8\omega_0}c_3a^3 + \frac{1}{2\omega_0}c_5\sin\gamma_1 = 0. \tag{15}$$

From (14) and (15), the so-called frequency-response equation is obtained:

$$\left[\frac{1}{4}c_1^2\cos^2\omega_0\tau + \left(\sigma + \frac{1}{2}c_1\sin\omega_0\tau + \frac{3}{8\omega_0}c_3a^2\right)^2\right]a^2 - \frac{1}{4\omega_0^2}c_5^2 = 0. \tag{16}$$

The amplitude of the response is a function of the external detuning, the feedback gains, the time delay, the coefficient of cubic term, and the amplitude of the external excitation.

The stability properties of a constant solution are examined by applying the classical method of linearization. We superpose small perturbations in the steady-state solution and then the resulting equations are linearized. Subsequently, we consider the eigenvalues of the corresponding system of first-order differential equations with constant coefficients, the Jacobian matrix. The eigenvalues of the Jacobian matrix satisfy the equation

$$\lambda^2 + R_1\lambda + R_2 = 0, \tag{17}$$

where R_1 and R_2 are functions of the parameters a_0, c_1, c_3, c_5, τ, and ω_0. From the Routh-Hurwitz criterion the steady-state solution is asymptotically stable if and only if R_1 and R_2 are greater than zero.

2.2. Subharmonic Resonance

For obtaining the averaging equations corresponding to the subharmonic resonance of order one-fourth ($\omega = 4\omega_0 + \varepsilon\sigma_1$), we take only the terms which do not contain the time in (9) and (10). Then we obtain

$$\omega_0\dot{a} = \varepsilon\left[-c_1 a\omega_0\cos\omega_0\tau - \frac{1}{16}c_6a^3\cos\gamma_2\right], \tag{18}$$

$$\omega_0 a(\varepsilon\sigma_1 - \dot{\varphi}) = \varepsilon\left[-\frac{1}{2}c_1a\omega_0\sin\omega_0\tau - \frac{3}{8}c_3a^3 - \frac{1}{16}c_6a^3\sin\gamma_2\right], \tag{19}$$

where

$$\gamma_2 = (\omega - 4\omega_0)t - \varphi = \varepsilon\sigma_1 t - \varphi. \tag{20}$$

Obviously, the presence of the feedback gains and time delay modifies the averaged equations by adding terms that are relevant to feedback control. Thus, it is possible to achieve the desirable behaviour if the feedback is deliberately implemented.

For steady-state solutions, we put $\dot{a} = \dot{\gamma}_2 = 0$; then (18) and (19) become

$$\frac{1}{2}c_1 a\cos\omega_0\tau + \frac{1}{16\omega_0}c_6a^3\cos\gamma_2 = 0, \tag{21}$$

$$\sigma_1 a + \frac{1}{2}c_1a\sin\omega_0\tau + \frac{3}{8\omega_0}c_3a^3 + \frac{1}{16\omega_0}c_6a^3\sin\gamma_2 = 0. \tag{22}$$

Equations (21) and (22) show that there are two possibilities: $a = 0$ or $a \neq 0$. When $a \neq 0$,

$$c_1\cos\omega_0\tau + \frac{1}{8\omega_0}c_6a^2\cos\gamma_2 = 0, \tag{23}$$

$$\frac{1}{2}\sigma_1 + c_1\sin\omega_0\tau + \frac{3}{4\omega_0}c_3a^2 + \frac{1}{8\omega_0}c_6a^2\sin\gamma_2 = 0. \tag{24}$$

From (23) and (24), the so-called frequency response equation is obtained:

$$c_1^2\cos^2\omega_0\tau + \left(\frac{1}{2}\sigma_1 + c_1\sin\omega_0\tau + \frac{3}{4\omega_0}c_3a^2\right)^2 - \frac{1}{64\omega_0^2}c_6^2a^4 = 0. \tag{25}$$

The amplitude of the response is a function of the external detuning, the feedback gains, the time delay, the coefficient of cubic term, and the amplitude of the parametric excitation.

Following the same analysis as in the above section, we can study the problem of stability.

3. The Method of Multiple Scales

To apply the method of multiple scales [43, 44], we introduce the nondimensional parameter $\varepsilon \ll 1$ for bookkeeping purposes, and define the fast time scale $T_0 = t$ and the slow time scales $T_1 = \varepsilon t$. Consequently, the time derivative becomes $\mathrm{d}/\mathrm{d}t = D_0 + \varepsilon D_1 + \cdots$, where $D_n = \partial/\partial T_n$. It is convenient to write the solution of (9) in the complex form

$$y(t;\varepsilon) = y_0(T_0,T_1,T_2,\ldots) + \varepsilon y_1(T_0,T_1,T_2,\ldots). \quad (26)$$

We note that the number of independent time scales needed depends on the order to which the expansion is carried out. If the expansion is carried out to $O(\varepsilon)$, then T_0 and T_1 are needed. Substituting (26) into (1) and equating the coefficient of like power of ε yields the following equations to order $O(1)$ and to order $O(\varepsilon)$:

$$O(1) : D_0^2 y_0 + \omega_0^2 y_0 = 0, \quad (27)$$

$$\begin{aligned} O(\varepsilon) : D_0^2 y_1 + \omega_0^2 y_1 &= -2D_0 D_1 y_0 \\ &- D_0 y_0(t-\tau) + c_3 y_0^3 + \frac{1}{2} c_4 y_0 \exp(\mathrm{i}\omega t) \\ &+ \frac{1}{2\mathrm{i}}(c_5 + c_6 y_0^3)\exp(\mathrm{i}\omega t). \end{aligned} \quad (28)$$

With this approach it turns out to be convenient to write the solution of (27) in the form

$$y_0 = A(T_0,T_1)\exp(\mathrm{i}\omega_0 T_0) + \bar{A}(T_0,T_1)\exp(-\mathrm{i}\omega_0 T_0), \quad (29)$$

where $\bar{A}$ is the complex conjugate of A, and the function A is still arbitrary at this level of approximation; it is determined by eliminating the secular terms at the higher levels of approximation.

Substituting y_0 into equation (28), we have

$$\begin{aligned} &D_0^2 y_1 + \omega_0^2 y_1 = \\ &\left\{\mathrm{i}\omega_0(-2D_1 A - c_1 A \exp(-\mathrm{i}\omega_0\tau)) + 3c_3 A^2 \bar{A}\right\} \\ &\cdot \exp(\mathrm{i}\omega_0 T_0) + \frac{1}{2} c_4 \bar{A} \exp\{\mathrm{i}(\omega - \omega_0) T_0\} \\ &- \frac{1}{2}\mathrm{i}\{c_5 + 3c_6 A\bar{A}^2 \exp(-\mathrm{i}\omega_0 T_0) \\ &+ c_6 \bar{A}^3 \exp(-3\mathrm{i}\omega_0 T_0)\}\exp(\mathrm{i}\omega T_0). \end{aligned} \quad (30)$$

Any particular solution of (30) contains secular or small divisor terms depending on the resonances that are considered. The general case in which all the above resonances occur simultaneously is considered next. The detuning parameters σ and σ_1 are first introduced according to

$$\omega = \omega_0 + \varepsilon\sigma, \quad \omega = 4\omega_0 + \varepsilon\sigma_1. \quad (31)$$

Then, inserting (31) into (30), we find that the secular terms are eliminated from y_1 if

$$\begin{aligned} &\mathrm{i}\omega_0(-2D_1 A - c_1 A \exp(-\mathrm{i}\omega_0\tau)) + 3c_3 A^2 \bar{A} \\ &+ \frac{1}{2}\mathrm{i}c_5 \bar{A} \exp(\mathrm{i}\sigma T_1) + \frac{1}{2}\mathrm{i}c_6 \bar{A}^3 \exp(\mathrm{i}\sigma_1 T_1) = 0. \end{aligned} \quad (32)$$

Substituting y by $1/2a\exp(\mathrm{i}\beta)$, where a and β are real functions, separating the real and imaginary parts, we obtain the first reduced modulation equations of amplitude and phase in the polar form:

$$a' = \frac{1}{2}c_1 a \cos\omega_0\tau - \frac{3}{2\omega_0}c_5 \cos\theta_1 - \frac{1}{16\omega_0}c_6 a^3 \cos\theta_2, \quad (33)$$

$$\begin{aligned} a\beta' = &-\frac{1}{2}c_1 a \sin\omega_0\tau \frac{3}{8\omega_0}c_3 a^3 \\ &- \frac{1}{2\omega_0}c_5 \sin\theta_1 + \frac{1}{16\omega_0}c_6 a^3 \sin\theta_2, \end{aligned} \quad (34)$$

where

$$\theta_1 = \sigma_1 T_1 - \beta, \quad \theta_2 = \sigma_2 T_1 - 4\beta. \quad (35)$$

To have stationary solutions for the system of equations (33) and (34), the following conditions must be satisfied:

$$a' = 0, \quad \theta_1 = \theta_2 = 0. \quad (36)$$

It follows from (36) that

$$\beta' = \sigma_1 = \frac{1}{4}\sigma_2 = \sigma. \quad (37)$$

Hence, the stationary solutions are given by

$$\frac{1}{2}c_1 a \cos\omega_0\tau - \frac{3}{2\omega_0}c_5 \cos\theta_1 - \frac{1}{16\omega_0}c_6 a^3 \cos\theta_2 = 0, \quad (38)$$

$$\begin{aligned} &a\sigma + \frac{1}{2}c_1 a \sin\omega_0\tau \frac{3}{8\omega_0}c_3 a^3 - \frac{1}{2\omega_0}c_5 \sin\theta_1 \\ &- \frac{1}{16\omega_0}c_6 a^3 \sin\theta_2 = 0. \end{aligned} \quad (39)$$

Two cases of resonance are considered as described in the following sections.

3.1. Primary Resonance

In the case of primary resonance (33) and (34) reduce to

$$\frac{1}{2}c_1 a\cos\omega_0\tau - \frac{3}{2\omega_0}c_5\cos\theta_1 = 0, \tag{40}$$

$$a\sigma + \frac{1}{2}c_1 a\sin\omega_0\tau\frac{3}{8\omega_0}c_3a^3 - \frac{1}{2\omega_0}c_5\sin\theta_1 = 0. \tag{41}$$

Eliminating θ_1 from (40) and (41) yields the frequency response equation

$$\left[\frac{1}{4}c_1^2\cos^2\omega_0\tau + \left(\sigma + \frac{1}{2}c_1\sin\omega_0\tau + \frac{3}{8\omega_0}c_3a^2\right)^2\right]a^2 - \frac{1}{4\omega_0^2}c_5^2 = 0, \tag{42}$$

which is in excellent agreement with (16) obtained by using the method of averaging.

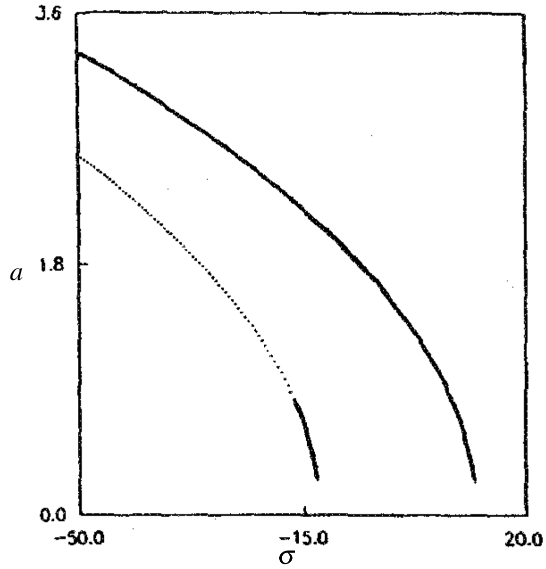

Fig. 1. Theoretical frequency-response curves of primary resonance.

3.2. Subharmonic Resonance

In the case of subharmonic resonance (33) and (34) reduce to

$$\frac{1}{2}c_1 a\cos\omega_0\tau - \frac{1}{16\omega_0}c_6a^3\cos\theta_2 = 0, \tag{43}$$

$$\frac{1}{4}\sigma_2 a + \frac{1}{2}c_1 a\sin\omega_0\tau\frac{3}{8\omega_0}c_3a^3 + \frac{1}{16\omega_0}c_6a^3\sin\theta_2 = 0. \tag{44}$$

There are two possibilities. First, $a = 0$; this is the linear case. Second, $a \neq 0$ and (43) and (44) yield the frequency response equation

$$c_1^2\cos^2\omega_0\tau + \left(\frac{1}{2}\sigma_1 + c_1\sin\omega_0\tau + \frac{3}{4\omega_0}c_3a^2\right)^2 - \frac{1}{64\omega_0^2}c_6^2a^4 = 0, \tag{45}$$

which is in excellent agreement with (25) obtained by using the method of averaging.

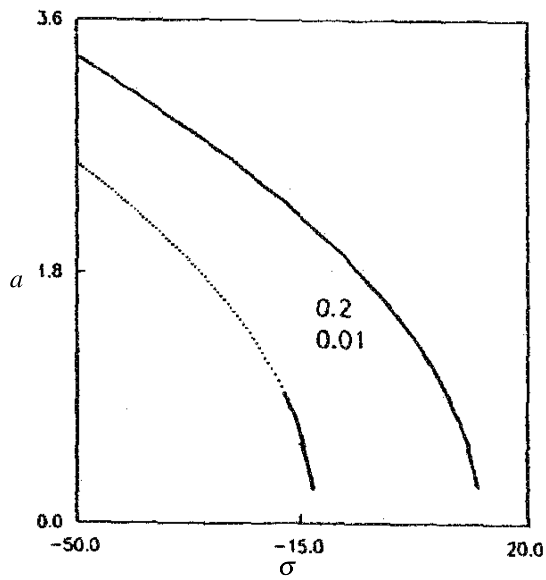

Fig. 2. Theoretical frequency-response curves if the damping factor c_1 is 0.01.

4. Numerical Results

The analytical analysis is presented graphically using the numerical method. The frequency-response equations (16) and (25) for the two cases (primary and subharmonic resonances) are nonlinear algebraic equations in the amplitude a. We focus our attention on the positive roots of these equations. A series of frequency-response diagrams is presented in Figures 1 – 18. The stability of a fixed point solution is studied by examination of the eigenvalues of the Jacobian matrix of (11) and (12) for primary resonance and (18) and (19) for

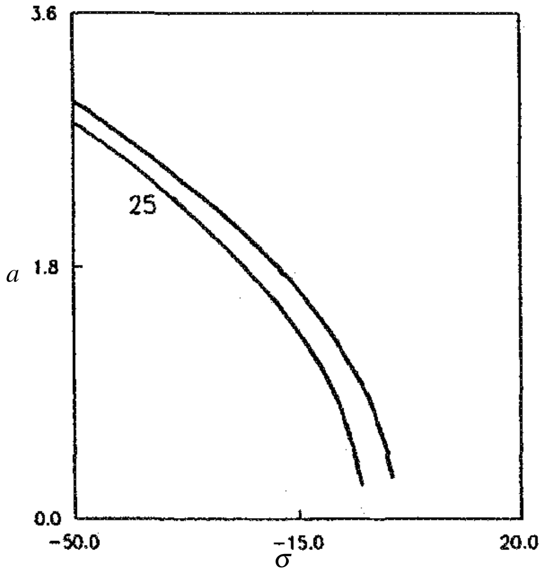

Fig. 3. Theoretical frequency-response curves if the damping factor c_1 is 25.

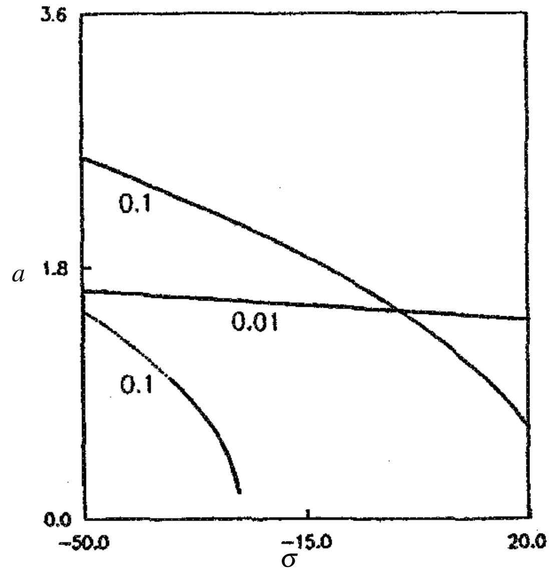

Fig. 5. Theoretical frequency-response curves for decreasing the natural frequency ω.

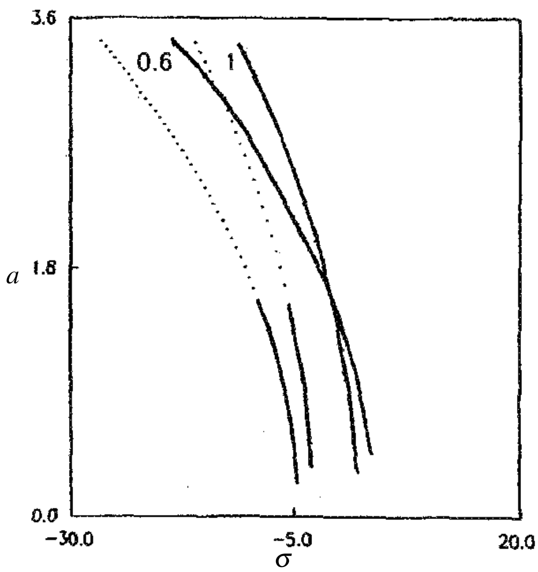

Fig. 4. Theoretical frequency-response curves for increasing the natural frequency ω.

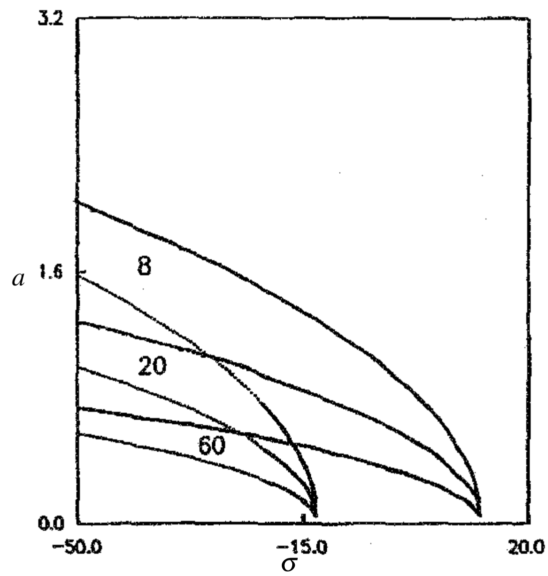

Fig. 6. Theoretical frequency-response curves for increasing the coefficient of the cubic term c_3.

subharmonic resonance evaluated at the fixed point. If the eigenvalues have negative real parts, then the fixed point is expected to it. These solutions are called stable nodes and are denoted by solid lines in the frequency-response curves of the figures. If pure real eigenvalues become positive, the fixed points lose stability and the motion is expected to diverge from it. These unstable solutions are saddles and are denoted by broken lines in the figures.

Figures 1 – 10 represent the frequency-response curves for primary resonance. In Figure 1, the response amplitude consists of two curves which bend to the left and have softening behaviour. The upper curve has a stable solution and the lower curve has stable and

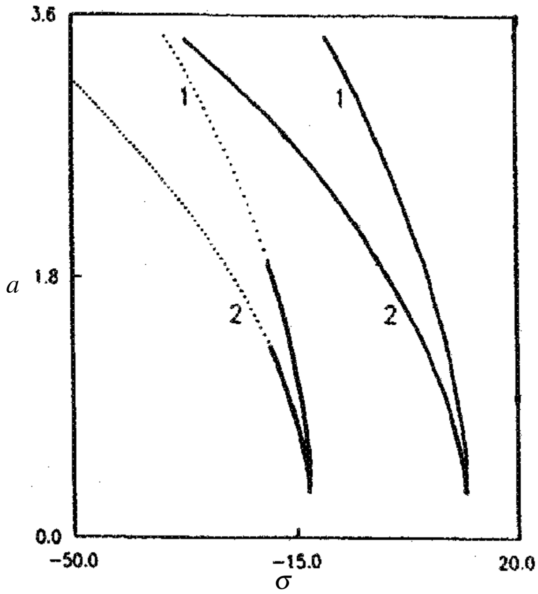

Fig. 7. Theoretical frequency-response curves for decreasing the coefficient of the cubic term c_3.

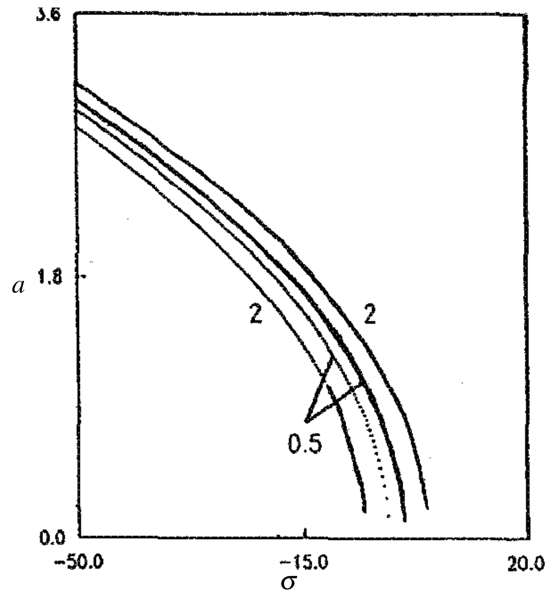

Fig. 9. Theoretical frequency-response curves for increasing the coefficient of the external excitation c_5.

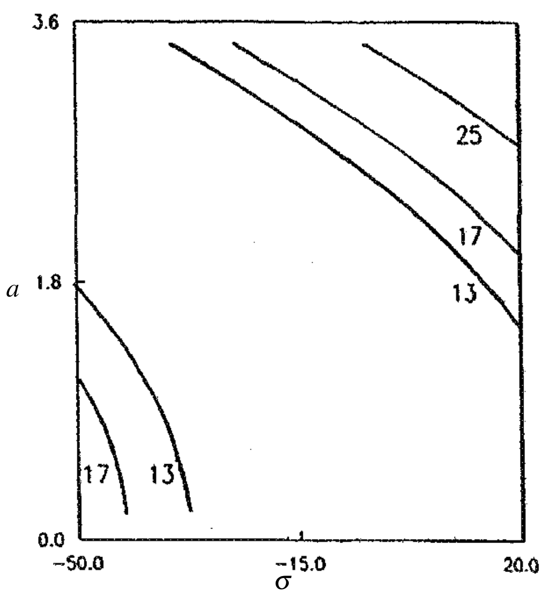

Fig. 8. Theoretical frequency-response curves for increasing the coefficient of the external excitation c_5.

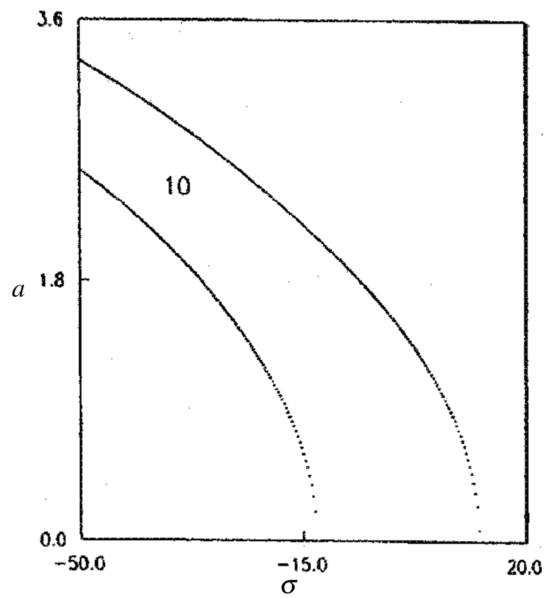

Fig. 10. Theoretical frequency-response curves if the time delay τ is 10.

unstable solutions, and there exists saddle-node bifurcation. When $c_1 = 0.01$ (Fig. 2), we note that the response amplitude is not affected and has the same magnitude so that the region of stability of the lower curve is increased. For increasing the damping factor c_1 up to 25 (Fig. 3), we note that the lower curve shifts upwards with increased stable magnitudes and the upper curve shifts downwards with decreased stable magnitudes. The zones of definition and multivalued are decreased and increased, respectively. When the natural frequency ω increases (Fig. 4), we note that the two curves contract and the regions of definition, multival-

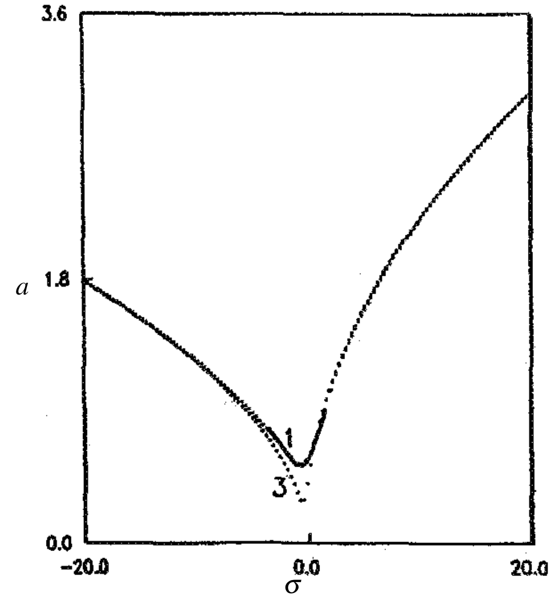

Fig. 11. Theoretical frequency-response curves for subharmonic resonance and if the time delay τ is 3.

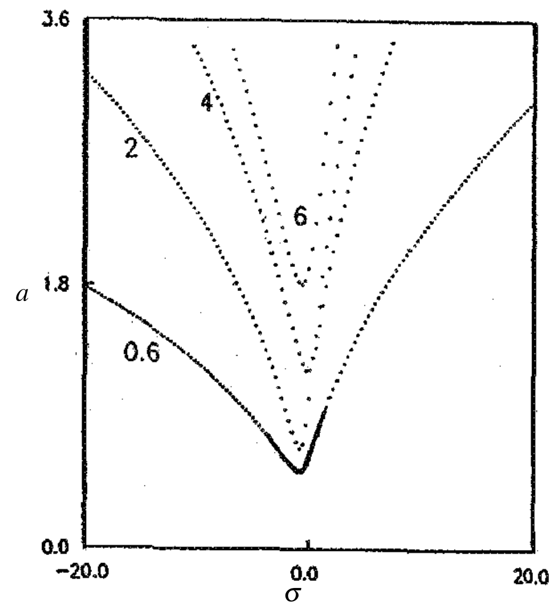

Fig. 12. Theoretical frequency-response curves for increasing the neutral frequency ω.

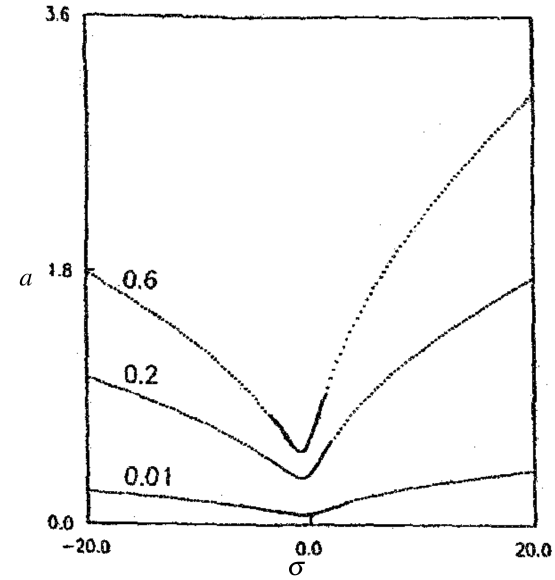

Fig. 13. Theoretical frequency-response curves for decreasing the neutral frequency ω.

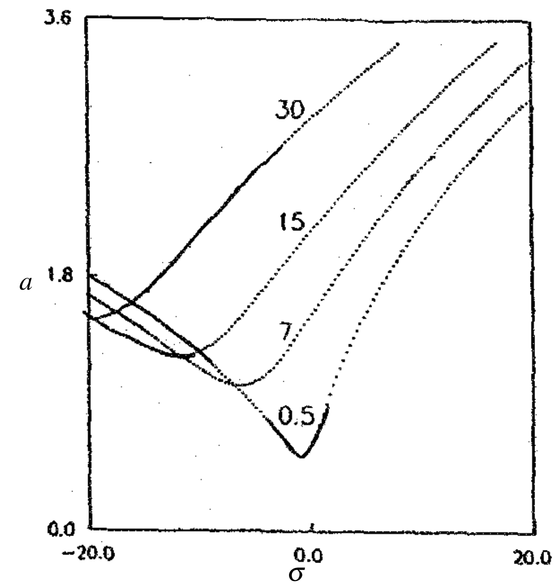

Fig. 14. Theoretical frequency-response curves increasing the damping factor c_1.

ued, and stability are decreased. As ω decreases further up to 0.01 (Fig. 5), the lower curve and the multivalued disappear. The zones of definition and stability are decreased. For increasing coefficient of the cubic term c_3, the two curves shift downwards with decreased magnitudes and have the same region of definition (Fig. 6). When the coefficient of the cubic term c_3 decreases (Fig. 7), we note that the two curves shift to the right with increased magnitudes. The region of stability of the left curve increases and the region of definition of the right curve decreases. As the coefficient of the external excitation c_5 takes the values 13 and 17

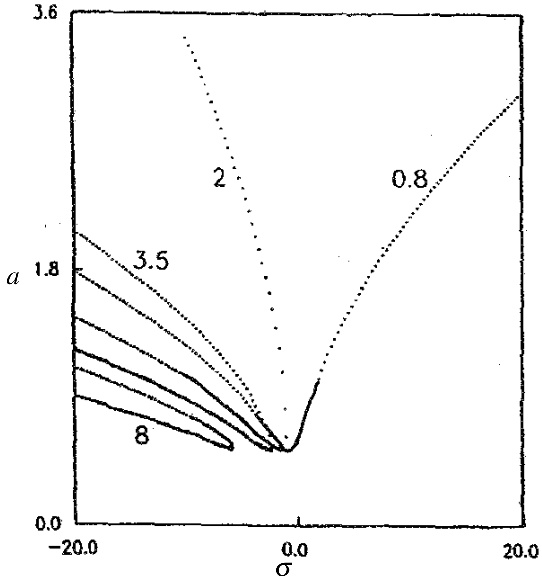

Fig. 15. Theoretical frequency-response curves for increasing the coefficient of the cubic term c_3.

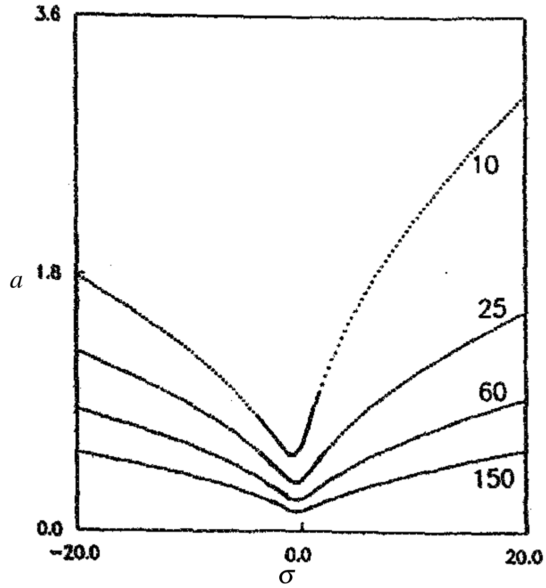

Fig. 17. Theoretical frequency-response curves for increasing the coefficient of the parametric excitation c_6.

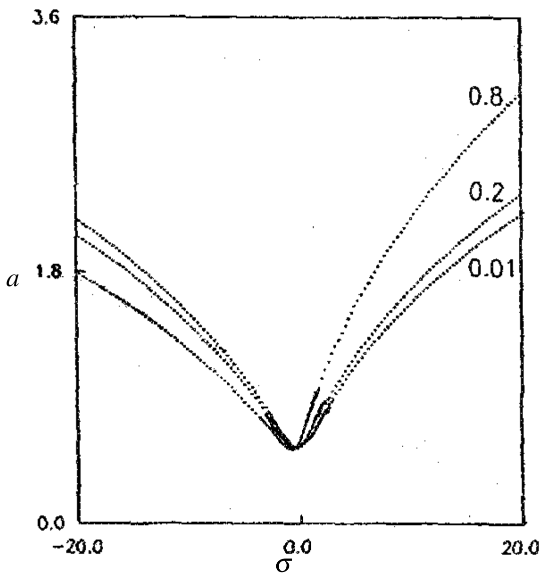

Fig. 16. Theoretical frequency-response curves for decreasing the coefficient of the cubic term c_3.

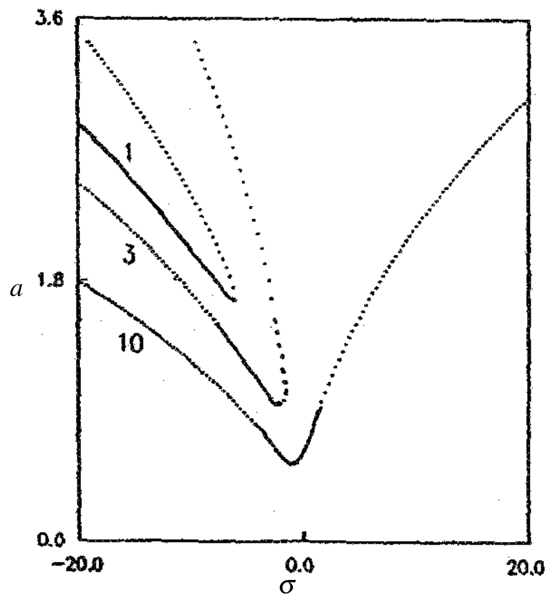

Fig. 18. Theoretical frequency-response curves for increasing the coefficient of the parametric excitation c_6.

(Fig. 8), we note that the left curve shifts downwards with decreased magnitudes and in a small interval. The right curve shifts upwards with increased magnitudes. When $c_5 = 25$, the left curve disappears and the right curve shifts upwards with increased stable magnitudes. Decreasing c_5 up to 2 (Fig. 9), the left curve shifts to the right with decreased stable magnitudes and the right curve shifts to the left with decreased magnitudes. The zone of definition is decreased. When $c_5 = 0.5$, we get the same variation as for $c_5 = 2$, but the left curve loses stability. When the time delay τ is increased, we get the same variation as in Figure 1 so that the two curves lose stability (Fig. 10).

Figures 11 – 18 represent the frequency-response curves for subharmonic resonance. In Fig. 11, the response amplitude has a single-valued curve which has the minimum value nearest to $\sigma_1 = 0$. There exist stable and unstable solution. When the time delay τ decreases, the response amplitude loses stability and the minimum value shifts downwards with decreased magnitudes. When the natural frequency ω decreases up to 2, the response amplitude shifts upwards with increased unstable magnitudes and the region of definition is decreased. When ω takes the values 4 and 6, the response amplitude is contracted, shifts upwards, and has increased unstable magnitudes, respectively (Fig. 12). As ω decreases the single-valued curve shifts downwards and has decreased magnitudes, respectively (Fig. 13). Increasing the damping factor c_1 (Fig. 14), the single-valued curve shifts upwards with increased magnitudes and the regions of stability and definition are increased and decreased, respectively. Increasing the coefficient of the cubic term c_3 (Fig. 15), we note that the right branch of the single-valued curve shifts to the left and there exists multivalued. The region of definition is decreased. When $c_3 = 3.5$, the response amplitude is semi-oval and the region of stability increases. When c_3 increases up to 8, the semi-oval shifts downwards with decreased magnitudes. When c_3 takes the values 0.2 and 0.01 (Fig. 16), the left and right branches of the single-valued curve shift upwards and downwards with decreased magnitudes, respectively. When the coefficient of the parametric excitation c_6 is increased, the single-valued curve shifts downwards with decreased magnitudes (Fig. 17). When $c_6 = 3$ (Fig. 18), we note that the right branch of the single-valued curve shifts to the left and there exists multivalued. The zone of definition is decreased. For decreasing c_6 up to 1, the response amplitude is semi-oval and shifts upwards with increased magnitudes. The regions of definition and stability are decreased and increased, respectively.

5. Conclusions

Here we present an analytical and numerical study of primary and subharmonic resonances of a nonlinear single-degree-of-freedom system under feedback control with a time delay. The concept of equivalent damping related to the delay feedback is proposed, and the appropriate choice of the feedback gains and the time delay is discussed. Both external (forcing) and parametric excitations are included. By means of the averaging method and the multiple scales method, two slow-flow equations for the amplitude and phase of the primary and subharmonic resonances and all other parameters are obtained. The steady-state (fixed points) corresponding to a periodic motion of the starting system is investigated and we show the frequency-response curves. We analyze the effect of time delay and other parameters on these oscillations. The stability of the fixed points is examined using the variational method. Numerical solutions are carried out and graphical representations of the results are presented and discussed. The present results reveal the following features of the steady-state response:

– From the analytical study we note that the results obtained by the two methods are in excellent agreement.
– From the frequency-response curves of primary resonance we observe that the response amplitude is not affected and has the same magnitudes when $c_1 = 0.01$. The region of definition decreases and increases for increasing ω. The lower curve disappears and the upper curve shifts upwards with increased stable magnitudes when $c_3 = 25$. When the time delay τ increases, the two curves have the same magnitudes and lose stability.
– From the frequency-response curves of primary resonance we observe that the response amplitude loses stability for increasing time delay τ. The response amplitude contracts with unstable magnitudes around $\sigma_1 = 0$. The zone of definition decreases for increasing the parameters ω, c_1, c_3, and c_6. The response amplitude is semi-oval when c_3 takes the values 3.5 and 8.

[1] K. Gopalsamy, Stability and Oscillations in Delay Differential Equations of Population Dynamics, Kluwer, Dordrecht 1992.
[2] Y. Kuang, Delay Differential Equations with Applications in Population Dynamics, Academic Press, New York 1993.
[3] Y. Kuang, Delay Differential Equations with Application in Population Dynamics, Springer, New York 2002.
[4] R.H. Plaut and J.C. Hsieh, J. Sound Vib. **114**, 73 (1987).

[5] R.H. Plaut and J.C. Hsieh, J. Sound Vib. **117**, 497 (1987).
[6] M. Abdel-Rohman, J. Eng. Mech. ASCE **113**, 1709 (1987).
[7] L.L. Chung, R.C. Lin, T.T. Soong, and A.M. Reinhorn, J. Eng. Mech. ASCE **115**, 1609 (1989).
[8] J.-P. Pu and J. M. Kelly, J. Eng. Mech. ASCE **117**, 2221 (1991).
[9] L. Palkovics and P.J.Th. Venhovens, Vehicle Syst. Dyn. **21**, 269 (1992).
[10] A.K. Agrawal, Y. Fujino, and B. Bhartia, Earthquake Eng. Struct. Dyn. **22**, 211 (1993).
[11] J.L. Moiola, A.G. Chiacchiarini, and A.C. Desages, Int. J. Bifurcation Chaos **6**, 661 (1996).
[12] J. Xu and J. Jiang, Chaos, Solitons, and Fractals **7**, 3 (1996).
[13] H. Yabuno, Nonlinear Dyn. **12**, 263 (1997).
[14] H. Yabuno, Nonlinear Dyn. **12**, 236 (1997).
[15] H. Hu, E. H. Dowell, and L. N. Virgin, Nonlinear Dyn. **15**, 311 (1998).
[16] H. Hu and Z. H. Wang, J. Sound Vib. **214**, 213 (1998).
[17] F. M. Atay, J. Sound Vib. **218**, 333 (1998).
[18] A. Hegazi, H. N. Agiza, and M. M. El-Dessok, Chaos, Solitons, and Fractals **12**, 631 (2001).
[19] J. C. Ji, Nonlinear Dyn. **25**, 369 (2001).
[20] A. Maccari, Nonlinear Dyn. **26**, 105 (2001).
[21] J. C. Ji and T. Leung, J. Sound Vib. **253**, 985 (2002).
[22] J.C. Ji and A.Y. T. Leung, Nonlinear Dyn. **27**, 411 (2002).
[23] M.S. Fofana and P.B. Ryba, Int. J. Nonlinear Mech. **39**, 79 (2004).
[24] M. Peng, Chaos, Solitons, and Fractals **25**, 1131 (2005).
[25] J.H. Park, Chaos, Solitons, and Fractals **23**, 503 (2005).
[26] Z. Liu and R. Yuan, Chaos, Solitons, and Fractals **23**, 551 (2005).
[27] M.T. Yassen, Chaos, Solitons, and Fractals **26**, 913 (2005).
[28] H. Wang and J. Liu, Chaos, Solitons, and Fractals **26**, 813 (2005).
[29] A. F. El-Bassiouny, Shock Vibr. **13**, 65 (2006).
[30] A. F. El-Bassiouny, Z. Naturforsch. **61a**, 629 (2006).
[31] Z. Sun, W. Xu, X. Yang, and T. Fang, Chaos, Solitons, and Fractals **31**, 39 (2007).
[32] A. F. El-Bassiouny, Phys. Scr. **75**, 726 (2006).
[33] A.F. El-Bassiouny, Mech. Res. Commun. **32**, 337 (2005).
[34] A.R.F. Elhefnawy and A.F. El-Bassiouny, Chaos, Solitons, and Fractals **23**, 289 (2005).
[35] A. F. El-Bassiouny, Chaos, Solitons, and Fractals **30**, 1098 (2006).
[36] A. F. El-Bassiouny, Phys. Scr. **74**, 39 (2006).
[37] A. M. Elnagger and A. F. El-Bassiouny. Bull. Sc. Assuit Univ. **24**, 25 (1995).
[38] A. F. El-Bassiouny, Appl. Math. Comput. **134**, 217 (2003).
[39] A. F. El-Bassiouny and M. Eissa, Phys. Scr. **70**, 101 (2004).
[40] A. F. El-Bassiouny, Phys. Scr. **72**, 203 (2005).
[41] A. M. Elnaggar and A. F. El-Bassiouny. Int. J. Theor. Phys. **31**, 1531 (1992).
[42] A. F. El-Bassiouny, Phys. Scr. **72**, 132 (2005).
[43] A. H. Nayfeh and D. T. Mook, Nonlinear Oscillations, Wiley, New York 1979.
[44] A. H. Nayfeh, Perturbation Techniques, Wiley, New York 1981.